Neutronics Design Flexibilities of the BigT Gadolinium Absorbers

Mohd-Syukri Yahya [a], Yonghee Kim [a*], and HyeongHeon Kim[b]
[a]*Department of Nuclear & Quantum Engineering, KAIST, Daejeon, Republic of Korea*
[b]*KEPCO Engineering & Construction Company (KEPCO E&C), Daejeon, Republic of Korea*
[*]*Corresponding author: yongheekim@kaist.ac.kr*

1. Introduction

Reactivity management of commercial Pressurized Water Reactors (PWRs) are typically performed with mechanical control rods, soluble boron and burnable absorbers (BA). Two most commonly used BA materials are boron and gadolinium (Gd). Boron has a moderately high thermal absorption cross-section. It therefore behaves like a $1/v$ "gray" volume absorber that becomes "whiter" with depletion. On the other hand, gadolinium has extremely high thermal absorption cross-section (65x than that of boron) such that it effectively prevents thermal neutrons from penetrating into a lumped gadolinium; i.e. gadolinium is essentially a thermally "black" surface absorber [1]. As a result, gadolinium is more sensitive than boron to self-shielding variation when lumped in a PWR lattice.

A new BA design named "Burnable absorber-Integrated Guide Thimble" (BigT) was recently proposed for PWR [2]. The BigT offers flexibility in BA self-shielding adjustment per design specifications. It is upon this assertion that this paper was prepared; i.e. this research aims to demonstrate the neutronics design flexibilities of BigT gadolinium absorbers. Specifically, three studies were completed to investigate sensitivities of the BigT gadolinium absorbers: (1) at a constant BA mass, (2) with a similar initial reactivity hold-down, and (3) for an optimal burnup reactivity swing.

2. The BigT Absorbers

The BigT absorber offers significant advances over state-of-the-art PWR thimble-occupying BA technology, in that it allows insertion of control rod in its thimble, is replaceable during refueling and is neutronically very flexible. Since it only requires minor modifications to the existing lattice design, the BigT is possibly retrofittable to most modern PWR technology.

While the BigT actually comes in three different design variants, this research focused on the BigT-AHR ('Azimuthally Heterogeneous Ring') concept only. The BigT-AHR, as depicted in Figure 1, is a zircaloy ring loaded into a standard guide thimble. The ring, which must be thin enough to enable insertion of control rod in its annulus hole, houses azimuthally-heterogeneous BA materials. One notes shape of the BA materials strongly affects its effectiveness as neutron poisons: a lumped BA with large *exposed* surface area has minimal self-shielding, and vice versa. In this research, the BA of choice is 100%TD (theoretical density) metallic Gd.

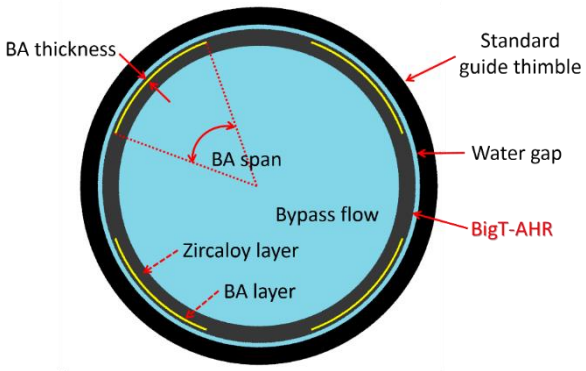

Fig. 1. Design concept of the BigT-AHR absorber.

3. The Simulation Parameters

Objective of this research was to demonstrate the neutronics design flexibilities of BigT Gd absorbers. The selected fuel assembly was ACE7 17x17 lattice design [3] as depicted in Figure 2. The lattice contains 4.95-w/o UO_2 fuel rods of 95%TD at 800K, cladding at 625K, and coolant without soluble boron and other materials (including BigT gadolinium absorbers) at 600K. Depletion calculations were performed for 510 EFPDs (effective full power days) at an average AP1000 lattice power of 54.14 kW/cm-lattice, which corresponds to a specific power of 37.4 W/g. All simulations were performed with 60,000 particles per cycle for 500x100 cycles by using Monte Carlo Serpent code [4] with ENDF/B-VII.0 nuclear data library.

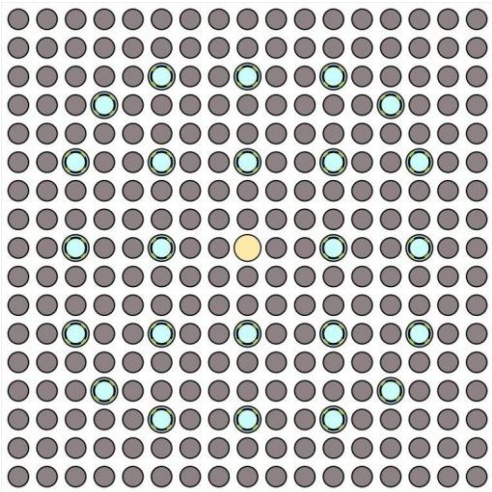

Fig. 2. Fully BigT-loaded 17x17 assembly lattice.

4. BigT Gadolinium Sensitivity Studies

Three sensitivity studies of the BigT gadolinium absorbers were performed, namely (1) constant gadolinium mass per BigT, (2) similar initial reactivity suppression, and (3) optimal burnup reactivity swing. In each study, three design variables of the BigT absorbers were methodically changed: gadolinium effective shapes, BigT loadings per lattice, and hybrid BigT designs. All studies are presented subsequently.

4.1 Sensitivities at the Same Gadolinium Mass per BigT

In this study, all 24 guide thimbles in the 17x17 lattice were loaded with BigT gadolinium absorbers, whose geometrical parameters are summarized in Table I. One notes the mass of gadolinium in this study was arbitrarily set constant at 0.1259 g per BigT, which was the required mass to suppress initial reactivity of '24 BigT-50' lattice ~13,000 pcm (k_∞ ~ 1.20), or ~93% hold-down in a non-poisoned lattice. Note that '24 BigT-50' is the 17x17 lattice loaded with 24 BigT gadolinium absorbers of 50° span. It is clear that at the same mass per BigT, a thicker gadolinium was required for a smaller-span rectangular pad. Meanwhile, aspect ratio is defined as the ratio of the two sides of a rectangle, with the longer side always in the numerator. A high aspect ratio represents a flattened rectangle, which has a correspondingly big *external* surface area.

Table I. Geometrical Parameters of Gadolinium in BigT Absorbers of Section 4.1

	Angular Span	Mass per BigT (g)	Thickness (mm)	Aspect Ratio
24 BigT-10	10°	0.1259	0.4869	1.7
24 BigT-30	30°	0.1259	0.1568	16.2
24 BigT-50	50°	0.1259	0.0935	45.6
24 BigT-70	70°	0.1259	0.0666	89.9
24 BigT-90	90°	0.1259	0.0517	149.0

4.1.1 Variation of Gadolinium Shapes

In this sub-study, shapes of gadolinium in the BigT absorbers were varied according to parameters tabulated in Table I. Figure 3 depicts the resulting reactivity depletion patterns over a 510-EFPD cycle of the different BigT designs. It is clear that a lattice loaded with a bigger gadolinium aspect ratio has a higher initial reactivity suppression and depletes faster (negative reactivity gradient), and vice versa. This is because a very big aspect ratio represents a very thin gadolinium block, essentially *exposing* more of the surface absorbers to thermal neutrons.

Figure 4 meanwhile depicts normalized pin powers of '24 BigT-90' lattice at BOC (beginning-of-cycle) and EOC (end-of-cycle). One notes that at BOC, the peaking hotspots occur at the lattice corners, and migrate towards the lattice center with burnup. Regardless, maximum normalized pin power is always recorded at BOC. The study also shows that a lattice with smaller initial reactivity suppression correspondingly yields a smaller peaking factor at BOC; i.e. peaking factor of '24 BigT-10' is the smallest, and that of '24 BigT-90' is the highest. This is because at BOC, the BigT absorbers suppress fission reactions at the lattice center, effectively forcing more fission reactions at the periphery to yield the preset lattice power. As BA is depleted, the corresponding fission suppression is likewise reduced, thereby gradually and uniformly diluting pin power throughout the lattice with burnup.

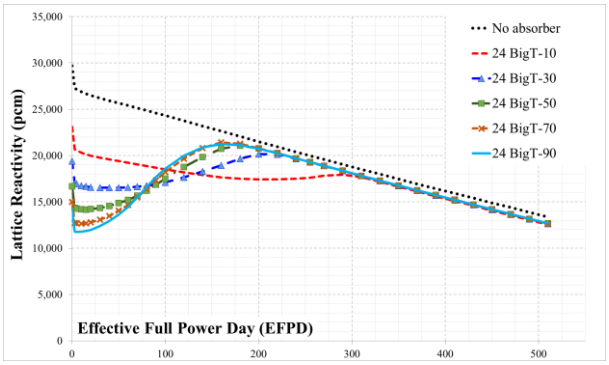

Fig. 3. Reactivity depletion of the BigT-loaded lattices simulated with different gadolinium shapes.

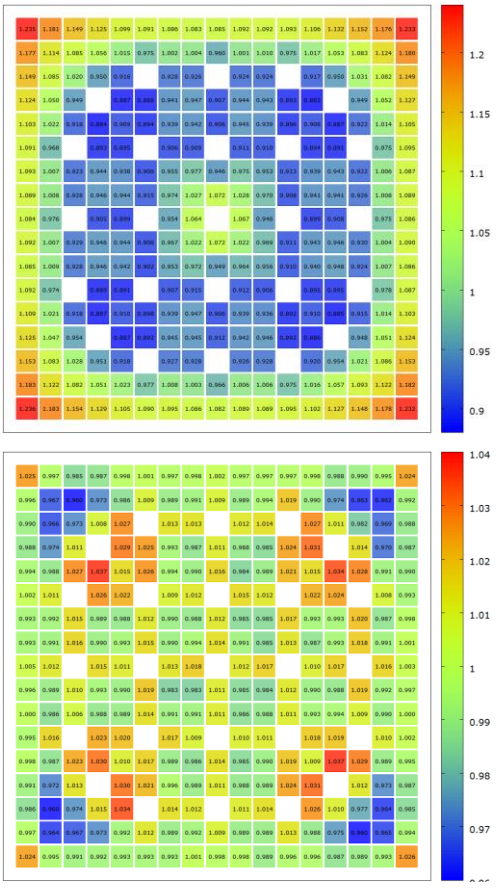

Fig. 4. Normalized pin power profiles of the '24 BigT-90' lattice; (top) at BOC, and (bottom) at EOC.

4.1.2 Variation of BigT loading-per-lattice

Gadolinium of '24 BigT-50' lattice listed in Table I was used throughout this sub-study. Instead of fully loading all 24 guide thimbles in the lattice with BigT gadolinium absorbers, some thimbles were left empty as water holes. Figure 5 depicts four possible BigT-loading variations, namely 8, 12, 16, and 20 BigT absorbers per lattice. One notes the BigT absorbers were symmetrically dispersed throughout the lattices, with absorber loading prioritized to thimbles nearby central pin clusters.

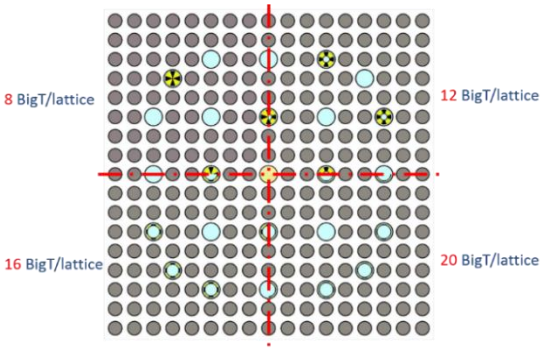

Fig. 5. Four variations of BigT loadings per lattice.

Figure 6 depicts the resulting reactivity depletions of different BigT loadings per lattice. It is clear the effect of removing BigT from the lattice is quite monotonous; i.e. smaller BigT loading results in smaller initial reactivity suppression and faster depletion. In fact, burnup reactivity swing of '8 BigT-50' lattice was noticeably quite flat. Interestingly, all lattices converged to ~22,000 pcm reactivity when almost all *surface* gadolinium had completely been depleted at ~175 EFPDs. In addition, all simulated lattices also ended with similar reactivity penalty, a consequence of residual poisonous tail of even-numbered gadolinium isotopes. The similarity is chiefly due to the similar degree of gadolinium self-shielding used in all simulated lattices. Meanwhile, the same pin power distribution pattern was observed with that of Section 4.1.1; i.e. smaller BigT loading per lattice translates to a correspondingly smaller reactivity suppression, resulting in a lower BOC peaking factor.

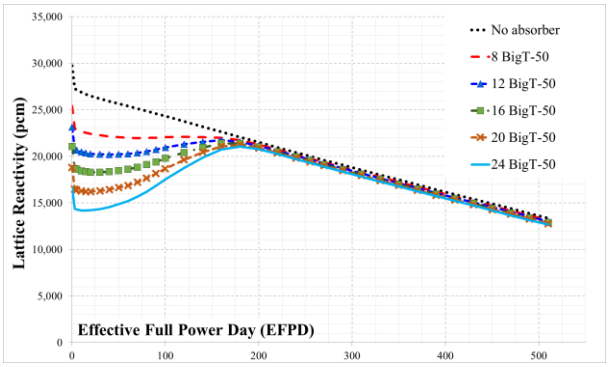

Fig. 6. Reactivity depletions of lattices with different BigT loadings at the same gadolinium mass per BigT.

4.1.3 Hybrid BigT Designs

In this sub-study, symmetrical combinations of different BigT absorbers in a lattice were simulated. Among the possible hybrid BigT designs are 12-12 or 8-8-8 variants, as depicted in Figure 7. '70-30' variant combines 12 BigT-70 and 12 BigT-30, with loading priority (i.e. central thimbles) given to the former. On the other hand, '10-50-90' variant loads 8 BigT-10, 8 BigT-50 and 8 BigT-90 absorbers. Different sequential arrangements are also possible. Gadolinium shapes listed in Table I were used throughout this sub-study.

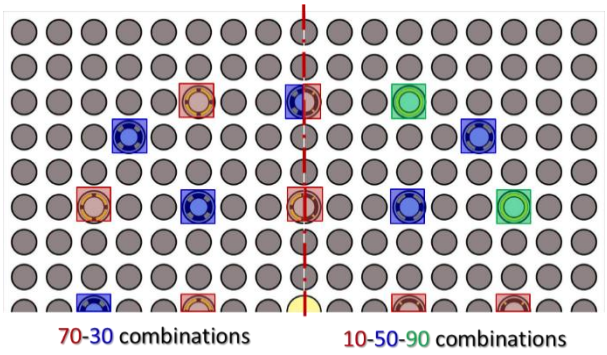

Fig. 7. Hybrid BigT designs: 12-12 and 8-8-8 variants.

Figure 8 shows the reactivity depletions of the selected hybrid BigT designs. It was quite difficult to ascertain patterns of the depletion. Upon closer inspection, it is however quite obvious that BigT absorbers loaded in central thimbles dominate the general depletion pattern. For example, while both '24 BigT 10-90' and '24 BigT-90-10' have similar initial reactivity suppressions, the former depletes slower (i.e. smaller reactivity gradient) since the BigT-90 absorbers, which has very high aspect ratio, are loaded in central thimbles and are, therefore, more dominant than BigT-10 absorbers. Similar observation is noted for the '24 BigT-30-70' and '24 BigT-70-30' variants. Meanwhile, depletion patterns in the hybrid 8-8-8 designs are less sensitive to the BigT location in the lattice; i.e. reactivity evolution is similar for any possible sequential arrangement of the hybrid BigT absorbers. Nonetheless, reactivity depletion of the hybrid designs somewhat balances patterns of the 'conventional' BigT absorbers. In Figure 8, EOC reactivity penalties of all hybrid BigT designs are also noticeably similar, except for that of '24 BigT 10-50-90' lattice. This is because the highly-self-shielded BigT-10 absorbers are dominant, such that it dramatically slows down overall depletion rate of the hybrid lattice to a point that some *surface* gadolinium was not completely depleted at EOC; hence the high tail of residual reactivity suppression. Meanwhile, BOC peaking factors of the hybrid BigT designs are quite similar to those of Section 4.1.1 (i.e. lattices fully-loaded with 'conventional' BigT absorbers).

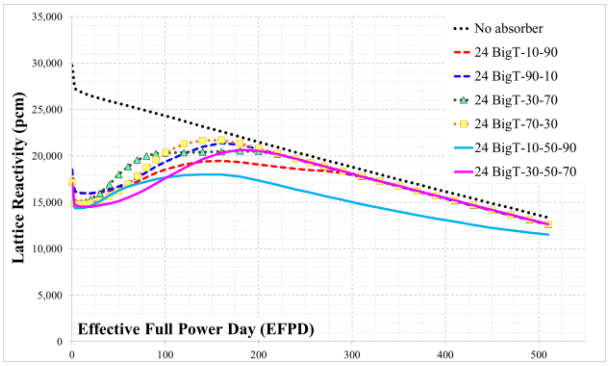

Fig. 8. Reactivity depletion of hybrid BigT designs.

Table II summarizes depletion results of Section 4.1. Initial suppression is defined as the reactivity differential between 'no absorber' and poisoned lattice at BOC, reactivity penalty is the same reactivity differential but at EOC, and the reactivity swing is reactivity range to completely deplete the *surface* gadolinium (i.e. prior to linear negative reactivity gradient). One notes with the same gadolinium mass per BigT, absorber shape significantly affects the initial reactivity suppression and the depletion rate; e.g. shape with a high aspect ratio has a big reactivity hold-down at BOC and depletes faster due to its huge *surface* area. In addition, a big loading of the BigT absorbers in the lattice increases the pin peaking factor at BOC.

Table II. Summary of the Neutronics Characteristics of Reactivity Depletion Patterns in Section 4.1

	Initial Suppression (pcm)	Reactivity Penalty (pcm)	Reactivity Swing (pcm)	BOC Peaking Factor
No absorber	29,710	0.0	13,930	1.048
24 BigT-10	-6,604	-813	3,241	1.124
24 BigT-30	-10,301	-703	3,629	1.165
24 BigT-50	-13,048	-688	6,881	1.206
24 BigT-70	-14,707	-709	8,751	1.226
24 BigT-90	-15,628	-684	9,502	1.236
8 BigT-50	-4,301	-227	1,279	1.080
12 BigT-50	-6,567	-340	1,531	1.119
16 BigT-50	-8,645	-460	3,120	1.137
20 BigT-50	-10,886	-579	5,039	1.167
24 BigT-10-90	-11,116	-767	3,498	1.180
24 BigT-90-10	-11,188	-755	5,390	1.183
24 BigT-30-70	-12,498	-720	5,616	1.195
24 BigT-70-30	-12,525	-717	6,905	1.203
24 BigT 10-50-90	-11,692	-722	4,485	1.182
24 BigT 30-50-70	-12,657	-700	6,136	1.194

4.2 Gadolinium Sensitivities for Similar Initial Reactivity Suppression

In this study, mass of gadolinium in BigT was adjusted to assure initial reactivity suppressions of the BigT-loaded lattices are ~13,000 pcm. Table III summarizes the resulting gadolinium geometrical parameters. It is obvious that a bigger gadolinium mass is required for a smaller-span BigT absorber and a smaller loading of BigT per lattice. The geometrical aspect ratios correspondingly vary with the variations of BigT shapes and loadings per lattice.

Table III. Geometrical Parameters of Gadolinium in BigT Absorbers of Section 4.2

	Angular Span	Mass per BigT (g)	Thickness (mm)	Aspect Ratio
24 BigT-10	10˚	0.4364	2.0171	3.0
24 BigT-30	30˚	0.3368	0.4317	5.7
24 BigT-50	50˚	0.1259	0.0935	45.6
24 BigT-70	70˚	0.0737	0.0389	154.4
24 BigT-90	90˚	0.0562	0.0230	335.6
8 BigT-50*	50˚	3.3282	4.5090	1.9
12 BigT-50	50˚	2.5669	2.5437	1.3
16 BigT-50	50˚	0.8605	0.6796	5.9
20 BigT-50	50˚	0.2976	0.2239	18.8

** 8 BigT-50 does not provide the required BOC reactivity suppression*

4.2.1 Variation of Gadolinium Shapes

Figure 9 depicts reactivity depletion of the BigT-loaded lattices with different gadolinium shapes which are designed to similarly suppress initial reactivity ~13,000 pcm. One notes the depicted depletion patterns are the exact opposite of the trends presented in Figure 3; higher gadolinium aspect ratio depletes faster instead. This is chiefly due to the bigger gadolinium content in the lattices loaded with smaller-span BigT absorbers (e.g. Big-10 and BigT-30), which subsequently results in possibly more neutron-gadolinium interactions.

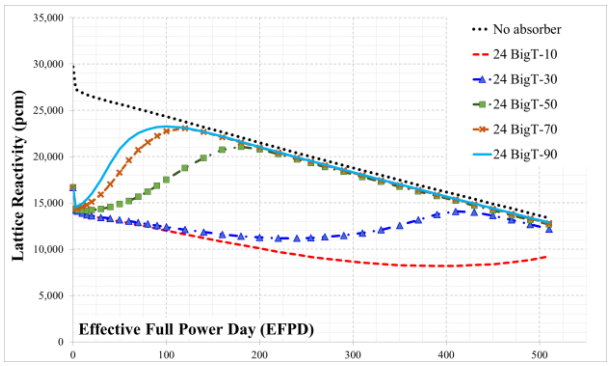

Fig. 9. Reactivity depletion of BigT-loaded lattices with different gadolinium shapes.

4.2.2 Variation of BigT Loadings per Lattice

Figure 10 depicts reactivity depletions of lattices with different BigT loadings which are designed to provide initial reactivity hold-down ~13,000 pcm. It is obvious that smaller BigT loading in the lattice requires bigger gadolinium content, thereby thickening the absorber shape and consequently increasing its self-shielding. As such, reactivity depletions of '8 BigT-50', '12 BigT-50' and '16 BigT-50' lattices are noticeably quite linear, providing clear evidences of very slow BA depletions.

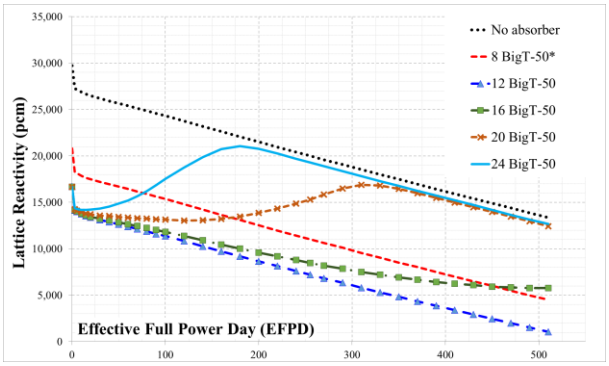

Fig. 10. Reactivity depletions of lattices with different BigT loadings.

4.2.3 Hybrid BigT Designs

Figure 11 depicts reactivity depletions of lattices loaded with hybrid BigT configurations; all designed to suppress initial reactivity ~13,000 pcm. Similar to the observation in Section 4.1.3, depletion of the hybrid BigT configuration somewhat balances its 'conventional' BigT designs. Interestingly, there are few noticeable double-hump depletion patterns, which are quite atypical for lumped gadolinium absorbers. This clearly demonstrates a unique feature of the hybrid BigT in adjusting the gadolinium self-shielding.

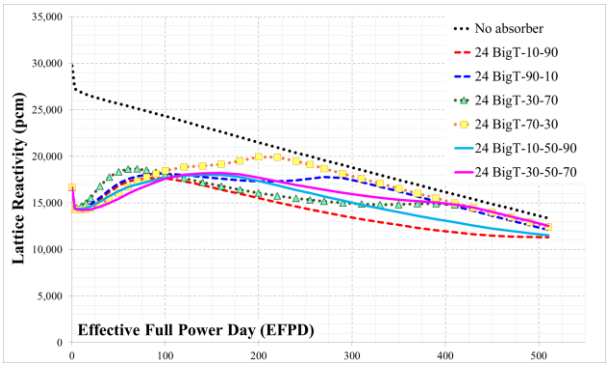

Fig. 11. Reactivity depletion of hybrid BigT designs.

Table IV summarizes neutronics characteristics of all reactivity depletions presented in Section 4.2. One notes BOC peaking factors in all lattices are quite similar (~1.20) regardless of the loaded BigT configurations. On the other hand, significant variations of reactivity penalties and swings were obtained, which noticeably decrease with absorber contents in the lattices.

Table IV. Summary of the Neutronics Characteristics of Reactivity Depletion Patterns in Section 4.2

	Initial Suppression (pcm)	Reactivity Penalty (pcm)	Reactivity Swing (pcm)	BOC Peaking Factor
No absorber	29,710	0.0	13,930	1.048
24 BigT-10	-13,025	-4,106	8,181	1.220
24 BigT-30	-13,037	-1,189	3,039	1.204
24 BigT-50	-13,048	-688	6,881	1.206
24 BigT-70	-13,049	-550	8,630	1.206
24 BigT-90	-13,027	-462	8,713	1.203
8 BigT-50*	-8,904*	-8,848	13,762	1.126
12 BigT-50	-12,993	-12,308	13,102	1.199
16 BigT-50	-13,053	-7,601	8,411	1.177
20 BigT-50	-13,039	-918	3,833	1.192
24 BigT-10-90	-13,025	-2,043	6,319	1.215
24 BigT-90-10	-13,038	-1,267	3,760	1.216
24 BigT-30-70	-13,058	-886	4,217	1.204
24 BigT-70-30	-13,032	-918	5,664	1.208
24 BigT 10-50-90	-13,034	-1,813	3,667	1.214
24 BigT 30-50-70	-13,024	-809	3,991	1.209

** 8 BigT-50 does not provide the required BOC reactivity suppression*

4.3. Gadolinium Sensitivities for Optimal Burnup Reactivity Swing

Objective of this study is to determine the optimal BigT configurations that yield minimum reactivity swing from initial suppression of ~13,000 pcm. While a big number of simulations were performed for the aforementioned purpose, this paper presents only the select few, as tabulated in Table V.

Table V. Geometrical Parameters of Gadolinium Metal in BigT Absorbers Simulated for Section 4.3.

	Angular Span	Mass per BigT (g)	Thickness (mm)	Aspect Ratio
24 BigT-30	30˚	0.3368	0.4317	5.7
20 BigT-45	45˚	0.3634	0.3064	12.3
16 BigT-80	80˚	0.4550	0.2138	31.5
24 BigT-30-40-50	30˚	0.3368	0.4317	5.7
	40˚	0.1984	0.1858	18.2
	50˚	0.1259	0.0935	45.6
24 BigT-30-35-40	30˚	0.3368	0.4317	5.7
	35˚	0.2582	0.2792	10.5
	40˚	0.1984	0.1858	18.2

Figure 12 depicts reactivity depletions of the selected BigT configurations. It is interesting to note that depletion pattern of '20 BigT-45' matches closely with that of '16 BigT-80' lattice. This subtly hints at another unique feature of the BigT concept: there are possibly more than one BigT gadolinium solutions to yield the same reactivity depletion pattern. This is another clear evidence of the BigT neutronics flexibilities.

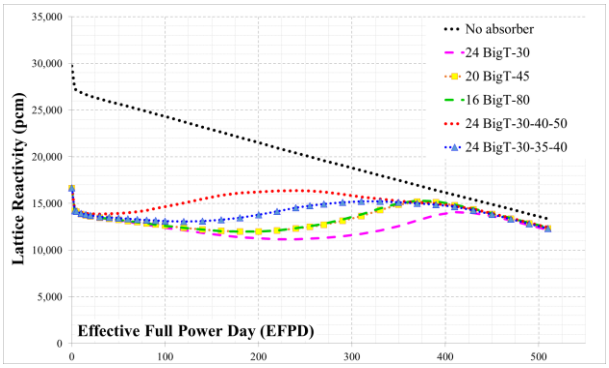

Fig. 12. Reactivity depletions of lattices with different BigT loadings.

Table VI summarizes neutronics characteristics of all reactivity depletions presented in Figure 12. The smallest reactivity swing from initial suppression of ~13,000 pcm was 2,173 pcm, obtained by loading the lattice with hybrid '24 Big 30-35-40' configuration. One must however note smaller swing may possibly be attained with further BigT optimization.

Table VI. Summary of the Neutronics Characteristics of Reactivity Depletion Patterns in Figure 12

	Initial Suppression (pcm)	Reactivity Penalty (pcm)	Reactivity Swing (pcm)	BOC Peaking Factor
No absorber	29,710	0.0	13,930	1.048
24 BigT-30	-13,037	-1,189	3,039	1.204
20 BigT-45	-13,077	-1,033	3,211	1.192
16 BigT-80	-13,028	-932	3,299	1.185
24 BigT 30-40-50	-13,017	-932	2,519	1.210
24 BigT 30-35-40	-13,037	-1,035	2,173	1.202

5. Conclusions

The paper clearly demonstrates neutronics flexibilities of the BigT gadolinium absorbers. Ascertained design variables are: (1) gadolinium effective shape, (2) BigT loading per lattice, and (3) BigT location in the lattice. Hybrid combination of the BigT designs may also alter the lattice depletion pattern, as well as density of gadolinium installed in the BigT absorbers. It is concluded that self-shielding of Gd can easily be adjusted in the BigT applications. Depending on the design requests, Gd-based BigT can provide both increasing and decreasing reactivity evolutions. In addition, a relatively flat reactivity change is also feasible with the BigT design optimization. For Gd depletion with small reactivity change, several BigT designs can also be synergistically combined in a single fuel assembly.

ACKNOWLEDGMENT

This work was supported by the Nuclear Power Core Technology Development Program of the Korea Institute of Energy Technology Evaluation and Planning (KETEP), granted financial resource from the Ministry of Trade, Industry & Energy, Republic of Korea. (20131610101850).

REFERENCES

[1] L. Goldstein and A. A. Strasser, "A Comparison of Gadolinia and Boron for Burnable Poison Applications in Pressurized Water Reactors," Nucl. Technol., 60, 352 (1983).
[2] Burnable Absorber-Integrated Control Rod Guide Thimble, Korean Patent No. 10-1497893, Republic of Korea (2015).
[3] Benchmark Matrix for Verification and Validation of the KARMA Code, Korea Atomic Energy Research Institute (KAERI), Republic of Korea (2010).
[4] J. Leppänen, Serpent – A Continuous-energy Monte Carlo Reactor Physics Burnup Calculation Code, VTT Technical Research Centre of Finland, Finland (2012).